ELSEVIER

International Journal of Psychophysiology 44 (2002) 143–163

INTERNATIONAL JOURNAL OF PSYCHOPHYSIOLOGY

www.elsevier.com/locate/ijpsycho

Phase-coupling of theta–gamma EEG rhythms during short-term memory processing

B. Schack[a,*], N. Vath[b], H. Petsche[c], H.-G. Geissler[d], E. Möller[a]

[a] *Institute of Medical Statistics, Computer Science and Documentation, University of Jena, Jahnstr. 3, D-07740 Jena, Germany*

[b] *Georg-Elias-Müller-Institute of Psychology, University of Goettingen, Goßlerstr. 14, D-37073 Goettingen, Germany*

[c] *Brain Research Institute, University of Vienna, Spitalgasse 4, A-1090 Vienna, Austria*

[d] *Institute of Psychology, University of Leipzig, Seeburgstr. 14-20, D-04103 Leipzig, Germany*

Received 5 June 2000; received in revised form 1 November 2001; accepted 6 November 2001

Abstract

Because of the importance of oscillations as a general phenomenon of neuronal activity the use of EEG spectral analysis is among the most important approaches for studying human information processing. Usually, oscillations at different frequencies occur simultaneously during information processing. Thus, the question for synchronisation of different frequencies by phase coupling and its possible functional significance is of primary importance. An answer may be given by bispectral analysis. Estimation of the (cross-) bispectrum allows to identify synchronised frequencies and possibly, the existence of non-linear phase coupling of different oscillators. Previous studies have demonstrated the simultaneous occurrence of slow (4–7 Hz) and fast (20–30 Hz) oscillations at frontal and prefrontal electrode positions during memory processing. However, interrelations between these rhythms have not been investigated up to now. In order to test short-term memory, the Sternberg task with random figures and number words was carried out on 10 female subjects. During the task EEG was recorded. Power and bispectral analyses from frontal, prefrontal and frontopolar regions were performed off-line. Increased power was found in both the theta and the gamma bands. Strong phase-coupling between theta at Fz and gamma at F3 and at Fp1, respectively, was shown for memorising number words by means of cross-bicoherence. A possible reason for this is an amplitude modulation of gamma frequencies by slow oscillations. The correspondent coherence analysis between the envelope of gamma frequencies at Fp1 and the raw EEG at Fz supports this presumption. This finding is interpreted as an EEG aspect of the functional linking between the prefrontal areas and the G.cinguli (as part of the limbic system), which are both extremely important for memory functions. © 2002 Elsevier Science B.V. All rights reserved.

Keywords: Memory; EEG; Oscillations; Theta band; Gamma band; Non-linear phase-coupling; Bispectral analysis

* Corresponding author. Tel.: +49-3641-933651; fax: +49-3641-933200.
E-mail address: schack@imsid.uni-jena.de (B. Schack).

0167-8760/02/$ - see front matter © 2002 Elsevier Science B.V. All rights reserved.
PII: S0167-8760(01)00199-4

1. Introduction

Oscillatory activity in different frequency bands of the EEG have long been known from various memory tasks. The role of oscillatory activity in the alpha and theta frequency bands has been explored in detail by Klimesch (1996, 1999).

In recent years, more and more relations have been found between memory processes and both theta and gamma oscillations. Klimesch and co-workers (Klimesch, 1996; Klimesch et al., 1997) found encoding and retrieval processes to be reflected by task-related increases in theta power. In 1999, Klimesch demonstrated an increase in theta band power in response to memory demands comparable to the behaviour of hippocampal theta in animals. Miller (1991) in his studies on animals, considered this theta rhythm as an oscillatory component of the hippocampal EEG related to memory processes. In man, Gevins et al. (1997) observed increased frontal midline theta rhythm with increased memory load.

Recent physiological studies in cats and monkeys (Singer, 1993; Eckhorn et al., 1993) reported synchronisation of gamma activity of cortical neurons during the processing of visual stimuli. Singer (1993) found that high-frequency oscillations in the beta and gamma ranges, i.e. at frequencies of 15–30 and 30–60 Hz, respectively, occur spontaneously in both man and higher mammals (cats and monkeys) when the subjects are in a state of focused attention. He demonstrated the functional significance of gamma oscillations in single unit recordings. Nakamura et al. (1992) observed both low- and high-frequency oscillations associated with a recognition task in the temporal pole of macaca mulatta.

In human brains, Singer (1993), Joliot et al. (1994) and Llinas et al. (1998) demonstrated spontaneous oscillatory electrical activity at frequencies at approximately 40 Hz. Its resetting by sensory stimulation has been proposed to be related to cognitive processing and to the temporal binding of sensory stimuli. Tallon-Baudry and co-workers (Tallon-Baudry et al., 1997, 1998; Tallon-Baudry and Bertrand, 1999) found induced gamma activity during the delay of a visual short-term memory task in humans.

Beyond indications that activity from both bands are involved in memory processing, there is a growing body of evidence indicating co-occurrence and even co-operation of theta and gamma oscillations in memory tasks. Co-occurrences in the EEG were shown by Sarnthein et al. (1998), who found that working memory activity involves synchronisation between prefrontal and posterior association cortex by phase-locked low-frequency (4–7 Hz) activity. In addition, they discovered enhanced coherence in the gamma range (19–32 Hz) between prefrontal and posterior association cortex during retention intervals. From coherence studies during various cognitive tasks, Petsche and Etlinger (1998) concluded that the frontopolar cortical regions play a significant role in short-term memory.

Approaches to explore in more detail, the relationships between activity in the alpha/theta and gamma bands were based upon behavioural analyses referring to Sternberg's item-recognition task (see Sternberg, 1975). From this task it could be concluded that operation times for recognition — depending on item complexity — vary between 20 and 80 ms/item, i.e. cycles of processing which, expressed in frequencies, correspond to the gamma and beta bands. Cavanagh (1972) relating these epochs to retention performance, found a direct proportionality to reciprocal memory spans. This yields, on average, a period of some 250 ms which becomes segmented in memory scanning, a period duration corresponding to theta oscillations. On the basis of these results physiological interpretations were proposed by Geissler and co-workers (Geissler, 1991, 1997; Geissler et al., 1999) and Lisman and co-workers (Lisman and Idiart, 1995; Jensen and Lisman, 1996, 1998). Whereas Geissler and co-workers centre upon relatively universal mechanisms of hierarchy formation among componential processes in perception and memory, the focus of Lisman and co-workers is the development of a specific multiplexing model explaining phase-coupled theta–gamma oscillations generated in the hippocampus.

Previous studies as mentioned above, showed that the location of gamma oscillations depends on the specificity of the cognitive task. Functional

imaging techniques such as positron emission tomography (PET) and functional magnetic resonance imaging (fMRI) are able to inform about the location of the activated cortex areas during memory tasks. Several recent neuroimaging studies suggest that prefrontal cortex is mainly involved in working memory.

A review of PET studies by Cabeza and Nyberg (1997) indicates the involvement of prefrontal cortex during information processing, among others: working memory; semantic memory retrieval; and episodic memory retrieval. A PET study by Tulving et al. (1994) demonstrates that left and right prefrontal lobes are part of an extensive neuronal network that subserves episodic memory. A preferential involvement of bilateral prefrontal cortex during episodic memory encoding and retrieval was also shown in a fMRI study by Iidaka et al. (1999). An activation of a common neural network for encoding was noticed regardless of the type of cognitive material presented in the left dorsal prefrontal cortex and the right cerebellum. In another fMRI study, Braver et al. (1997) showed that dorsolateral and left inferior regions of the prefrontal cortex exhibit a linear relationship between strength of activity and working memory load. Moreover, they identified additional brain regions showing a linear relationship with load, suggesting a distributed circuit in which the prefrontal cortex participates when working memory is involved. Petrides et al. (1993) observed in a PET study a strong bilateral activation within the mid-dorsolateral frontal cortex while maintaining numbers in working memory. In another PET study Swartz et al. (1991) examined abstract visual memory. They found that activations in the ventral premotor cortex and supramarginal and angular gyri were highly correlated with changes in the dorsolateral prefrontal cortex and also supported the role of the dorsal prefrontal region in non-spatial working memory in men.

Beside the general involvement of the prefrontal cortex in working memory the specificity of its different regions was investigated (Wilson et al., 1993; Goldman-Rakic, 1988, 1997; Paulesu et al., 1993; Shallice et al., 1994; Tulving et al., 1994; Iidaka et al., 1999; Smith et al., 1996). Other studies dealt with joint activations of cortex and hippocampus (Fernandez et al., 1999; Squire et al., 1992).

Up to now it is undecided whether phase-coupled theta-gamma oscillations do exist in the EEG of the prefrontal cortex, which would be associated to activities of neural networks during memory tasks. The bispectral analysis is a suitable methodical tool to investigate this question. The mathematical foundation of the definition and estimation of the spectral parameters of third order like (cross-) bispectrum, (cross-) biamplitude and (cross-) bicoherence is presented in detail in Nikias and Petropulu (1993). Additionally, our own methods of dynamic spectral analysis (Schack et al. 1999a,b,c; Möller et al. 1999) were used in order to examine temporal aspects. The definitions and estimation procedures of these methods will be given in Section 2.

Only recently several authors used the new tool of bispectral analysis for investigating the EEG. Jeffrey and Chamoun (1994) gave an introduction to this topic. By using this new tool, Schanze and Eckhorn (1997) found significant phase correlations between different frequencies in the visual cortex of the cat and monkey. Bullock et al. (1997) used bispectral analysis for the detection of short-term non-stationarity and non-linearity. Muthuswamy et al. (1999) detected phase coupling between two frequency components within the delta–theta frequency band of EEG bursts. Gajraj et al. (1998) applied the EEG bispectrum in order to distinguish the transition form unconsciousness to consciousness. Shils et al. (1996) studied the interactions between the electrocerebral activity resulting from stimulation of the left and right visual fields. He observed non-linear interactions between visual fields by means of bispectral analysis.

The main aim of this study is to test the general hypothesis of the existence of non-linear phase-coupled slow and fast rhythms within the frontal area during memory processing.

2. Methods and materials

2.1. Experiment and subjects

Ten healthy, female right-handed adults (age =

25–35 years) were performing the modified Sternberg task. Two different kinds of stimulus material served as items to be memorised: one-digit number words, zero, one, ..., nine (in German); and a set of 10 random figures. The figures were irregular rectangles of approximately the same area.

Sets with random set sizes 1, 2, 3 or 4 of words and random figures, respectively, were visually represented for 200 ms each followed by an interval of 1000 ms. A cross-symbol signalised the end of the presentation of the set. After another interval of 1800 ms for retention, a test figure or number word, respectively, was presented. The subjects had to press a 'yes' button if the probe corresponded to one of the elements of the presented set and a 'no' button if not (see Fig. 1).

The two different kinds of stimuli — number words and random figures — were presented in 12 alternating blocks, each block containing 64 tasks. Altogether, 768 tasks were performed per session and subject, in detail, 48 questions with positive probe per kind of stimuli and set size, and 48 questions with negative probe per kind of stimuli and set size. Two sessions on different days were carried out.

The EEG was registered during the presentation, retention and retrieval interval. The EEG was recorded from the scalp by means of 19 non-polarizable Ag–AgCl electrodes according to the international 10–20 system against linked ear lobes reference (impedance $< 5\ \mathrm{k}\Omega$, sampling frequency at 256 Hz). Their time constant of the recording device was 0.3 s and the upper frequency limit was 70 Hz. Simultaneously, the electro-oculogram (EOG) was recorded from two additional electrodes, one on the outer side of the eye and one above the eye. Eye-movements and blinks were removed by visual control by two independent, experienced researchers. Only trials without artefacts were included in further data-processing.

The number of artefact-free trials per session, set size, and item modality ranged between 60 and 85. The rest situation was recorded before the beginning of the task. Thirty trials of 2-s EEG epochs where selected for further analysis.

2.2. Mathematical methods

Several spectral functions of second and third order were used. The EEG records are understood as realisations of a multi-dimensional stochastic process.

2.2.1. Calculation of time-invariant spectral functions of second order: power and coherence spectra

In order to establish rhythmic activity and linear phase relations between rhythms of the same frequency at different sites on the scalp, ordinary power and coherence spectra were estimated by means of calculating and averaging the periodogram and cross-periodogram on the basis of Fourier transform (see e.g. Schack et al., 2000).

2.2.2. Calculation of time-invariant spectral functions of third order: cross-biamplitude and cross-bicoherence

From the ordinary power spectrum it cannot be decided whether phase coupling exists between different frequency components. For this purpose, the investigation of spectral functions of third order is needed in order to detect non-linear phase coupling between rhythms of possibly different frequencies within one or between two or three EEG channels. Bispectral analysis is the most qualified tool for analysing multiplicative connections between two rhythms, generating a third frequency component.

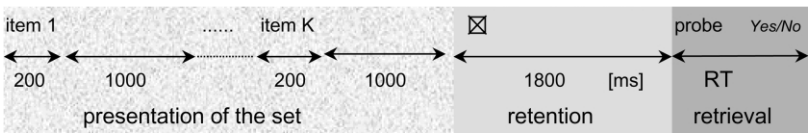

Fig. 1. Experimental design of the Sternberg paradigm.

The cross-bispectrum of three stationary signals $\{x(t)\}$, $\{y(t)\}$ and $\{z(t)\}$ is defined by

$$B(f_1,f_2) = \mathbf{E}[X(f_1)\cdot Y(f_2)\cdot Z^*(f_1+f_2)], \quad (1)$$

where $X(.)$, $Y(.)$ and $Z(.)$ denote the Fourier transforms of the signals $\{x(t)\}$, $\{y(t)\}$ and $\{z(t)\}$, *denotes the complex conjugate and **E** stands for the expectation value (Nikias and Petropulu (1993)). The cross-bispectrum is a two-dimensional complex function. In the special case of $\{y(t)\} = \{x(t)\}$ and $\{z(t)\} = \{x(t)\}$ it is called the bispectrum. The cross-biamplitude is the magnitude of the cross-bispectrum. The normalisation of the cross-biamplitude yields the cross-bicoherence according to Shils et al. (1996) and Kim and Powers (1979):

$$\Gamma(f_1,f_2) = \frac{|B(f_1,f_2)|}{\sqrt{\mathbf{E}|X(f_1)\cdot Y(f_2)|^2 \cdot \mathbf{E}|Z(f_1+f_2)|^2}}. \quad (2)$$

Nikias and Petropulu (1993) simply used the product of the power spectra at the frequencies f_1, f_2 and f_1+f_2 instead of the denominator in Eq. (2). The advantage of the definition above is the obvious interpretation as a correlation between the variables $X(f_1)\cdot Y(f_2)$ and $Z(f_1+f_2)$, and the normalisation property:$0 \le \Gamma(f_1,f_2) \le 1$.

The bispectral parameters (cross-)biamplitude and (cross-)bicoherence of three EEG signals are computed by direct estimation methods (Nikias and Petropulu, 1993). Let $[x^m(t_k)\ y^m(t_k)\ z^m(t_k)]_{k=0,1,\ldots N}$ be the sample values of three EEG channels of the mth trial, where $m = 1,...,M$. For the mth trial the following product of the correspondent Fourier transformations is calculated

$$B^m(f_1,f_2) = X^m(f_1)\cdot Y^m(f_2)\cdot Z^{m*}(f_1+f_2). \quad (3)$$

The (cross-)bispectrum is estimated by averaging over M trials:

$$\hat{B}(f_1,f_2) = \frac{1}{M}\sum_{m=1}^{M} B^m(f_1,f_2). \quad (4)$$

The (cross-)bicoherence is computed, respectively, as follows:

$$\hat{\Gamma}(f_1,f_2) = \frac{|\hat{B}(f_1,f_2)|}{\sqrt{\frac{1}{M}\sum_{m=1}^{M}|X^m(f_1)\cdot Y^m(f_2)|^2 \cdot \frac{1}{M}\sum_{m=1}^{M}|Z^m(f_1+f_2)|^2}} \quad (5)$$

In order to prove the existence of phase coupling between two different frequencies the significance test developed by Shils et al. (1996) was used. If

$$\hat{\Gamma}(f_1,f_2) > \frac{2}{\sqrt{M}} \quad (6)$$

the (cross-) bicoherence is different from zero with an error probability $\alpha \le 0.05$.

2.2.3. Calculation of time-variant spectral functions of second order: instantaneous power and coherence spectra

In order to consider the time development of the spectral functions power and coherence an adaptive estimation method is used, which allows a high time and frequency resolution. The basic idea of the method is as follows: a pair of EEG channels is understood as a two-dimensional instationary signal process. This process is modelled as a two-dimensional autoregressive moving-average (ARMA) model with time-dependent parameters. The optimisation criterion for adapting parameters is the minimisation of the prediction error of the model in the least mean square sense. The correction of the model according to this criterion is performed at every sample point. Thus, the parameters of the model are functions of time and allow the parametric calculation of the momentary spectral density matrix of the ARMA model, which approximates the spectral density matrix of the underlying pair of EEG channels for the momentary time-point. Subsequently, the continuous estimation of the power and coherence is derived from the momentary spectral density matrix of the fitted ARMA model.

Although the correction will be performed at every sample point, a smearing of the time evolution of the power and coherence estimation cannot be prevented. The continuous power and coherence estimation depends on the past with an exponentially decreasing memory. Nevertheless, the time resolution is much higher than that for estimation methods on the basis of the Fourier transformation. For considering a set of M trials, the time-dependent functions of coherence were averaged for each time-point.

In order to avoid an unlimited increase of instantaneous power in unstable states of single trials the adaptation procedure was modified in the univariate case. Instead of averaging the time-dependent power functions a joint ARMA model with time-dependent parameters was fitted to the whole set of trials.

The interested reader can find the detailed estimation procedures in Schack et al. (1999a,b,c) and in Möller et al. (1999, 2001).

2.2.4. Modelling of non-linear phase coupling by amplitude modulation

Time-continuous amplitude modulation of fast EEG rhythms by slow rhythms at the same or a different site of the cortex may lead to non-linear phase coupling. The amplitude modulation of fast rhythms can be described by means of the envelope of the correspondent band power and a time-variant coherence analysis between the envelope and the modulating slow rhythms. For estimation we used a consistent adaptive approach.

That means, for estimating the envelope, in a first step the signal $[x(n) = x(t_n)]_{n=0,1,\ldots}$ was filtered for a chosen frequency band by a finite impulse response (FIR) filter. Afterwards, the time-continuous power $[s(n) = s(t_n)]_{n=0,1,\ldots}$ of the filtered signal $[\tilde{x}(n) = \tilde{x}(t_n)]_{n=0,1,\ldots}$ was calculated according to the following adaptive estimation procedure:

$$s(0) = \tilde{x}^2(0)$$

$$s(n) = s(n-1) - c \cdot (s(n-1)) - \tilde{x}^2(n); \quad n = 1,2,... \tag{7}$$

where $c = 0.01$ (for details see Grieszbach et al., 1994). The root of the adaptively estimated instantaneous power of the filtered signal served as an estimation of the envelope:

$$e(n) = \sqrt{s(n)}; \quad n = 1,2,... \tag{8}$$

A phase coupling between slow oscillations of a modulating signal $[y^m(t_n)]_{n=0,1,\ldots}$ and the envelope $[e^m(n) = e^m(t_n)]_{n=0,1,\ldots}$ of fast oscillations of another signal $[x^m(t_n)]_{n=0,1,\ldots}$, may be described by instantaneous coherence analysis performed for all single trials, $m = 1,...,M$ and averaging thereafter.

3. Results

3.1. Behavioural data

The reaction times for both stimuli — number words and random figures — show the well-known dependence on the memory load (see Fig. 2). In all cases reaction time increases with increasing set size.

Memorisation of unfamiliar random figures evidently requires more time than memorisation of number words. The comparison of the reaction times of the first and the second run shows an obvious learning effect. The significance of these

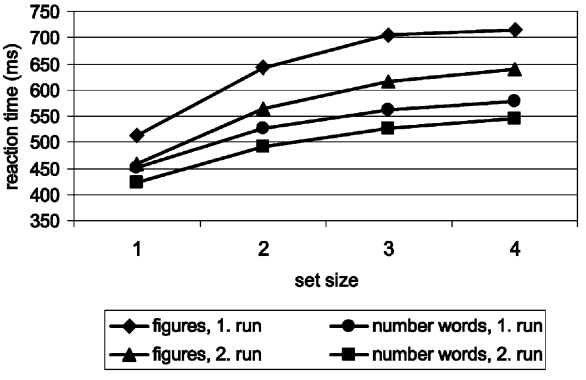

Fig. 2. Mean reaction times (10 subjects) in dependence of memory load for the Sternberg task with regard to the 1st and the 2nd run.

Table 1
Results of ANOVA for comparing reaction times with factors modality (words, pictures), run (first, second) and set size (1, 2, 3 and 4)

Reaction times		
Main effects	*F*-value	*P*-value
Modality	29.169	0.000
Run	13.858	0.000
Set size	27.948	0.000

results was proven by ANOVA with the factors modality, run and set size (see Table 1).

From shorter reaction times, it may be assumed that stronger results with respect to the investigation of memorising will be obtained from the second run. Further analysis is concentrated on data from the second run. Our main attention was paid to the experiments with high memory load, namely set sizes 3 and 4.

3.2. Spectral analysis of second order

In order to get information about general power distribution in the topographical context, power estimations were performed for the retention time interval of 1800 ms. The upper part of Fig. 3 shows the average of power spectra for 10 subjects in the case of memorising number words with set size 4.

Principally, the pictures for set size 3 and for memorising random figures (set sizes 3 and 4) are similar. In all cases, remarkably high-frequency oscillations (20–40 Hz) with high amplitudes are found in the left and right frontopolar areas. In all cases, both mean amplitudes as well as frequencies are higher in the left frontopolar electrode position. However, in two subjects the opposite was found with respect to gamma power at Fp1 and Fp2, namely a larger gamma power at Fp2. In all cases, gamma oscillations are spread over a broad frequency band. The frequencies with maximal gamma power vary inter-individually. The highest theta power (3–7 Hz) is found at the central electrode positions Fz and Cz. Alpha-oscillations (8–13 Hz) predominate in the parieto-occipital area (electrode positions P3, Pz, P4, O1 and O2) and spread out up to temporal and central regions. In order to show that high gamma power at Fp1 and Fp2 is not produced by microsaccades of the eyes, the mean power spectra of the two EOG channels were included in the lower part of Fig. 3. No gamma power is observable for the EOG.

Although the power spectra of Fp1 and Fp2 in Fig. 3 seem to be similar, there are some differences with regard to the modality of the items and also to the hemisphere. Fig. 4 presents a comparison of the power spectra of Fp1 and Fp2 for the situations of rest and memorising number words and random figures (both for set size 4).

The power spectra for memorising number words and random figures show the same high gamma power in Fp1 with the maximum at approximately 30–33 Hz (left upper panel). On the other hand, the frequency of maximal gamma power at Fp2 is lower for both tasks at approximately 25–30 Hz (right upper panel). During the rest situation, instead, a clear alpha-peak at 10 Hz appears in both frontopolar positions. A comparison of the power spectra of the left and right frontopolar electrode positions yields higher gamma power at Fp1 and higher frequencies of maximal gamma power for both modalities of items (lower left and right panels). These differences are more obvious in the case of memorising number words.

The power spectra at F7, F3, F4 and F8 show slightly increased gamma power (see Fig. 3). A possible interaction with regard to gamma activity within the frontal area was proven by means of common coherence analysis for the electrode pairs Fp1/F7, Fp1/F3, F7/F3, Fp2/F8, Fp2/F4 and F8/F4. The coherence values were negligible (significance level of 5%) for frequencies larger than 20 Hz in contrast to the slower frequency range.

Yet, common coherence analysis of second order does not allow to detect synchronisation of oscillations with different frequencies, which may be caused by interdependencies of different rhythms and/or non-linear phase coupling phenomena. To study this question was the aim of the following bispectral analysis.

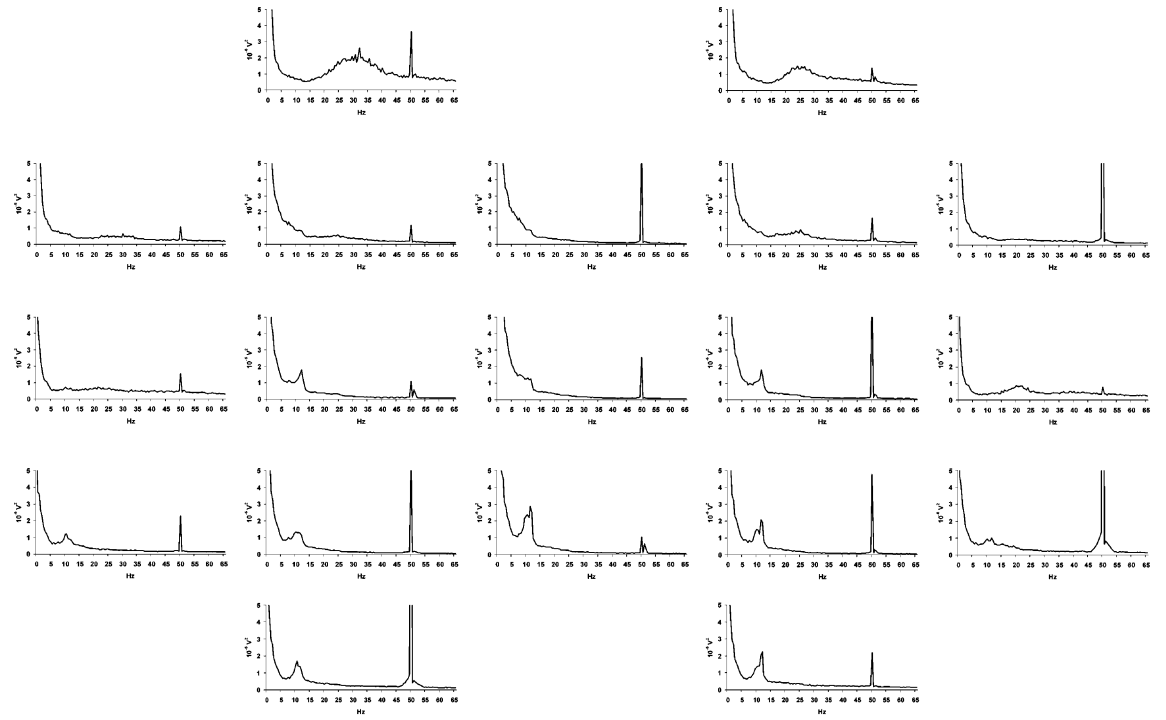

Scheme of electrode positions:

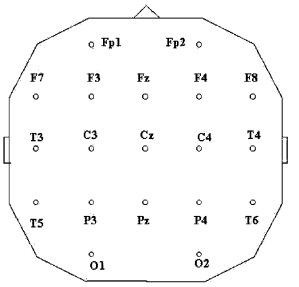

EOG 1

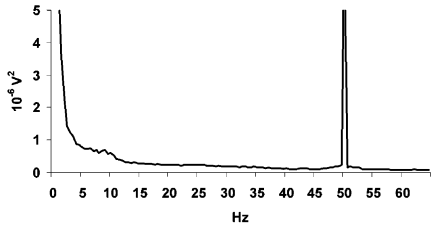

EOG 2

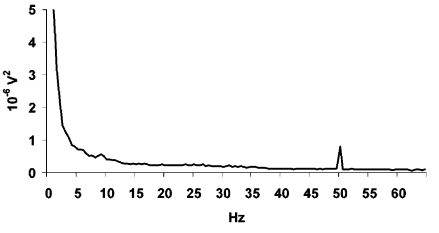

Fig. 3. Upper part: mean power spectra (10 subjects) for 19 electrode positions for the retention period for memorising number words with set size 4. The scheme at the bottom indicates the localisation of the corresponding electrode positions on the head. The high peak at 50 Hz is due to AC. Fast frequency oscillations with high amplitudes are only found in both frontopolar areas. Lower part: mean power spectra (10 subjects) for the two EOG channels for the same time interval.

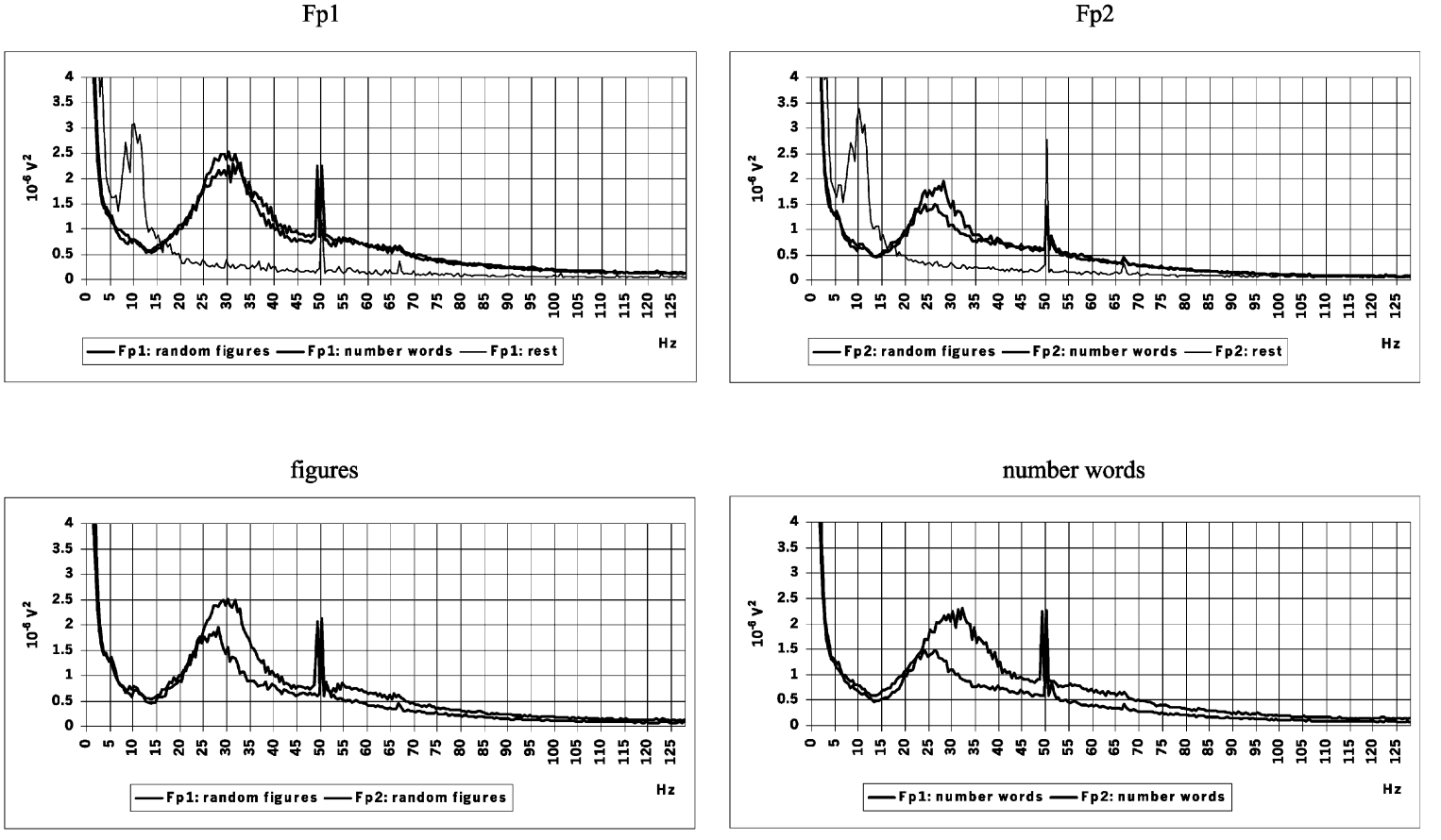

Fig. 4. Mean power spectra (10 subjects) for the frontopolar electrode positions Fp1 and Fp2 for the retention period (set size 4) and during the rest situation. Upper left: comparison of spectra on Fp1 during memorising random figures (grey), during memorising number words (black, bold) and during rest situation (black, thin). Upper right: comparison of spectra on Fp2 during memorising random figures (grey), during memorising number words (black, bold) and during rest situation (black, thin). Lower left: comparison of spectra on Fp1 (black) and Fp2 (grey) during memorising random figures. Lower right: comparison of spectra on Fp1 (black) and Fp2 (grey) during memorising number words.

3.3. Spectral analysis of third order

3.3.1. Bispectral analysis

Bispectral analysis allows the detection of interactions among rhythmic signals at different frequencies. As outlined in the introduction, we were in particular interested in possible interaction of fast oscillations (20–40 Hz) within the frontal area with slower oscillations.

In a first step biamplitudes were estimated according to Eqs. (3) and (4) (with $x = y = z$) for all 10 subjects during the retention period in the case of memorising number words with set size 4 for seven frontal electrode positions Fp1, Fp2, F7, F3, Fz, F4 and F8. High biamplitudes for fast oscillations (> 20 Hz) were found only for Fp1 and Fp2. Therefore, further analysis was concentrated on these two locations.

The calculation of biamplitudes was repeated for memorising number words with set size 3 and

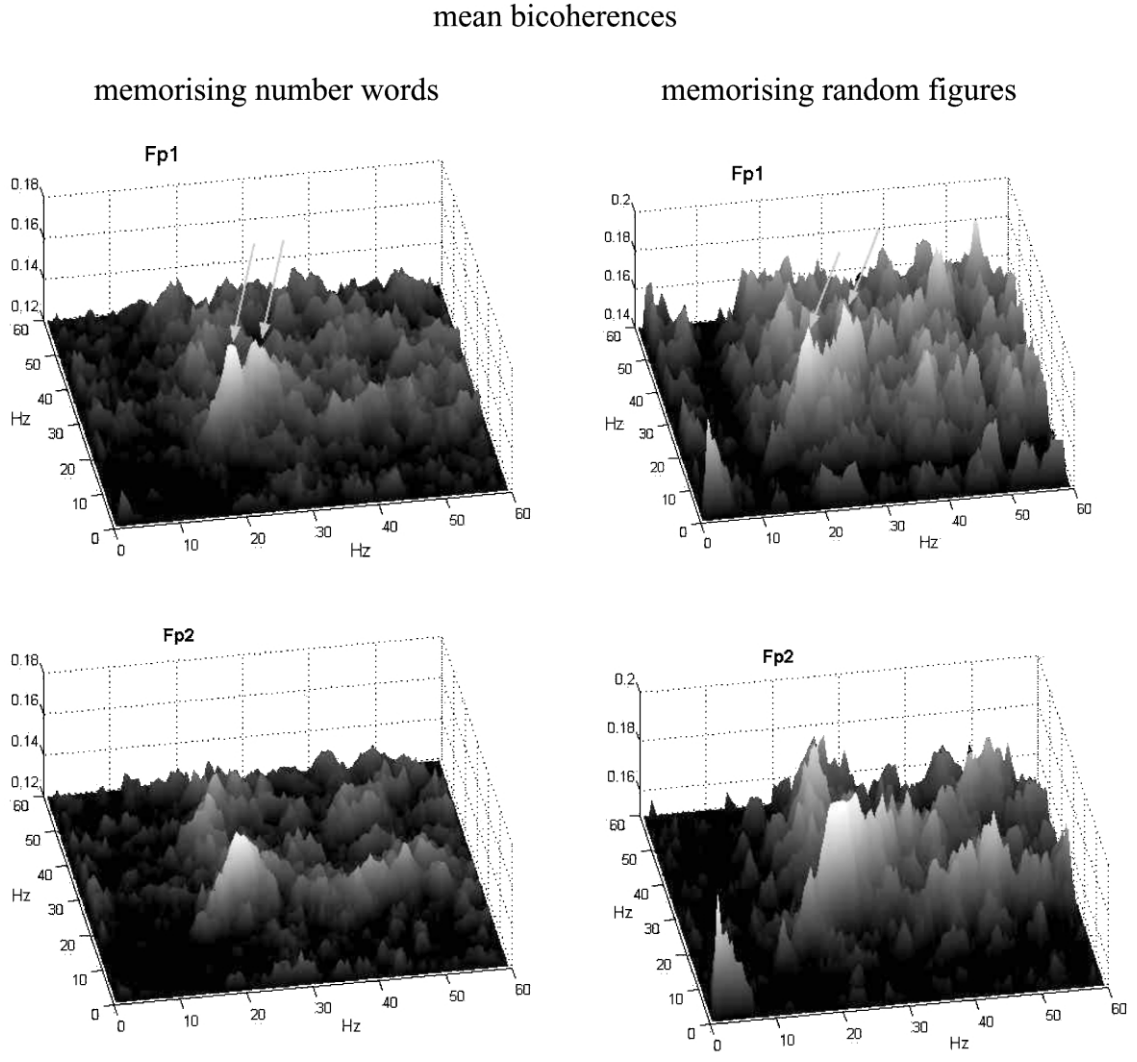

Fig. 5. Mean bicoherences (10 subjects) of Fp1 (upper row) and of Fp2 (lower row) during the retention period: left column: memorising number words; and right column: memorising random figures. The arrows indicate increased bicoherences at approximately 20 and 25 Hz at Fp1.

Table 2
Mean percentage of test positivity for non-zero bicoherence for selected frequency area [significance test according to Eq. (6) with α-level = 5%]

Frequency area (Hz)	Number words set size = 3		Random figures set size = 3		Number words set size = 4		Random figures set size = 4	
	Fp1	Fp2	Fp1	Fp2	Fp1	Fp2	Fp1	Fp2
20–25/ 20–25	**80%**	50%	**70%**	60%	**80%**	70%	**90%**	60%
25–30/ 25–30	**70%**	40%	**80%**	60%	**90%**	60%	**70%**	80%
3–7/ 25–30	30%	0%	40%	20%	40%	10%	20%	10%
20–25/ 45–50	40%	20%	50%	30%	70%	50%	70%	40%
15–20/ 35–40	50%	10%	40%	20%	60%	70%	60%	30%

for memorising figures with set sizes 3 and 4. High biamplitudes occurred for pairs of fast oscillations (> 20 Hz) and for pairs of slow (0–5 Hz) and fast (> 20 Hz) oscillations. However, the range of fast oscillations was broader (20–40 Hz) for Fp1 than for Fp2 (20–30 Hz). This fact agrees with the characteristics of the correspondent power spectra. The calculation of biamplitudes for set size 3 yielded the same results. During the rest situation high biamplitudes appeared only for delta- and alpha-oscillations.

Biamplitudes depend on amplitudes of oscillations and only point at common occurrence of oscillations with the respective frequency pair of the frequency plane. On the other hand, bicoherence is a normalised parameter and points out frequency pairs with real phase coupling. The result of bicoherence computation is shown in Fig. 5.

High bicoherences were obtained if the two frequencies were within the range of 20–30 Hz at Fp1 and of 20–25 Hz at Fp2. Furthermore, increased bicoherences occurred between frequencies within this range and multiple frequencies, probably due to ordinary phase coupling of oscillations with their first harmonic ones. This fact may explain the existence of relatively high power within the 40–60-Hz frequency range.

High bicoherences between fast frequencies and theta frequencies are not visible. Yet, one effect can be noted for electrode position Fp1: there are two clear peaks (marked by arrows in Fig. 5) of bicoherence within the paired frequency range of 20–30 Hz. Further, the distance of the peaks is approximately 5 Hz Hz in the case of memorising number words and larger in case of memorising random figures. The calculations for set size 3 yielded the same results. This observation hints to possibly interactions of fast frequencies at Fp1 and slow frequencies at other electrode positions, which would evoke the second peak with faster frequencies of bicoherence.

In order to test the significant difference of bicoherence values from zero the significance test according to Eq. (6) was performed for each of the four situations of memorising number words and random figures, each with set sizes 3 and 4 for all 10 subjects for 128/128 frequency pairs (frequency range = 0.5–64 Hz; frequency resolution = 0.5 Hz). The highest percentage values of test statistics were found around the frequency ranges (Hz) 20–25/20–25 and 25–30/25–30. Table 2 contains the occurrence of non-zero bicoherence with regard to the 10 subjects for the selected frequency ranges in percentages.

It is remarkable that for the frequency range 3–7 Hz/25–30 Hz, in all cases non-zero bicoherences appear more frequently at Fp1 than at Fp2. This fact suggests a possible influence of interactions between slow oscillations in neighboured frontal locations and fast oscillations at Fp1.

3.3.2. Cross-bispectral analysis

In order to detect phase coupling between oscillations at different frontal electrode positions cross-bispectral analysis according to Eqs. (3)–(6) was performed. From the results of bispectral analysis at Fp1 and Fp2 we were interested in looking for phase relations between slow rhythms at F3, Fz and fast rhythms at Fp1, as well as between slow rhythms at F4, Fz and fast rhythms at Fp2, respectively. Therefore, four types of channel triples with sample values $[x^m(t_k)\ y^m(t_k)\ y^m(t_k)]_{k=0,1,\ldots N}$, $m = 1,...,M$, were chosen: (F3, Fp1, Fp1), (Fz, Fp1, Fp1), (F4, Fp2, Fp2) and (Fz, Fp2, Fp2). The choice of such triplets where the second and the third channel are the same, allows the detection of phase-coupled oscillations between the first and second channel.

This strategy will be demonstrated for one subject for the channel triple (Fz, Fp1, Fp1) during memorising number words. Fig. 6 shows the cross-biamplitude with the correspondent power spectra at Fz and Fp1 for memorising number words with set size 3.

In contrast to biamplitude, the cross-biamplitude matrix (upper panel of Fig. 6) is not symmetrical. The horizontal direction indicates frequency components at Fz, whereas the vertical direction indicates frequency components at Fp1. High cross-biamplitudes may be observed within the frequency ranges 1–7 Hz at Fz and 1–5 Hz at Fp1, as well as in 1–7 Hz at Fz and 20–30 Hz at Fp1. High cross-biamplitudes at the vertical line for 50 Hz at Fz are caused by a technical artefact. The generation of high biamplitudes for the fre-

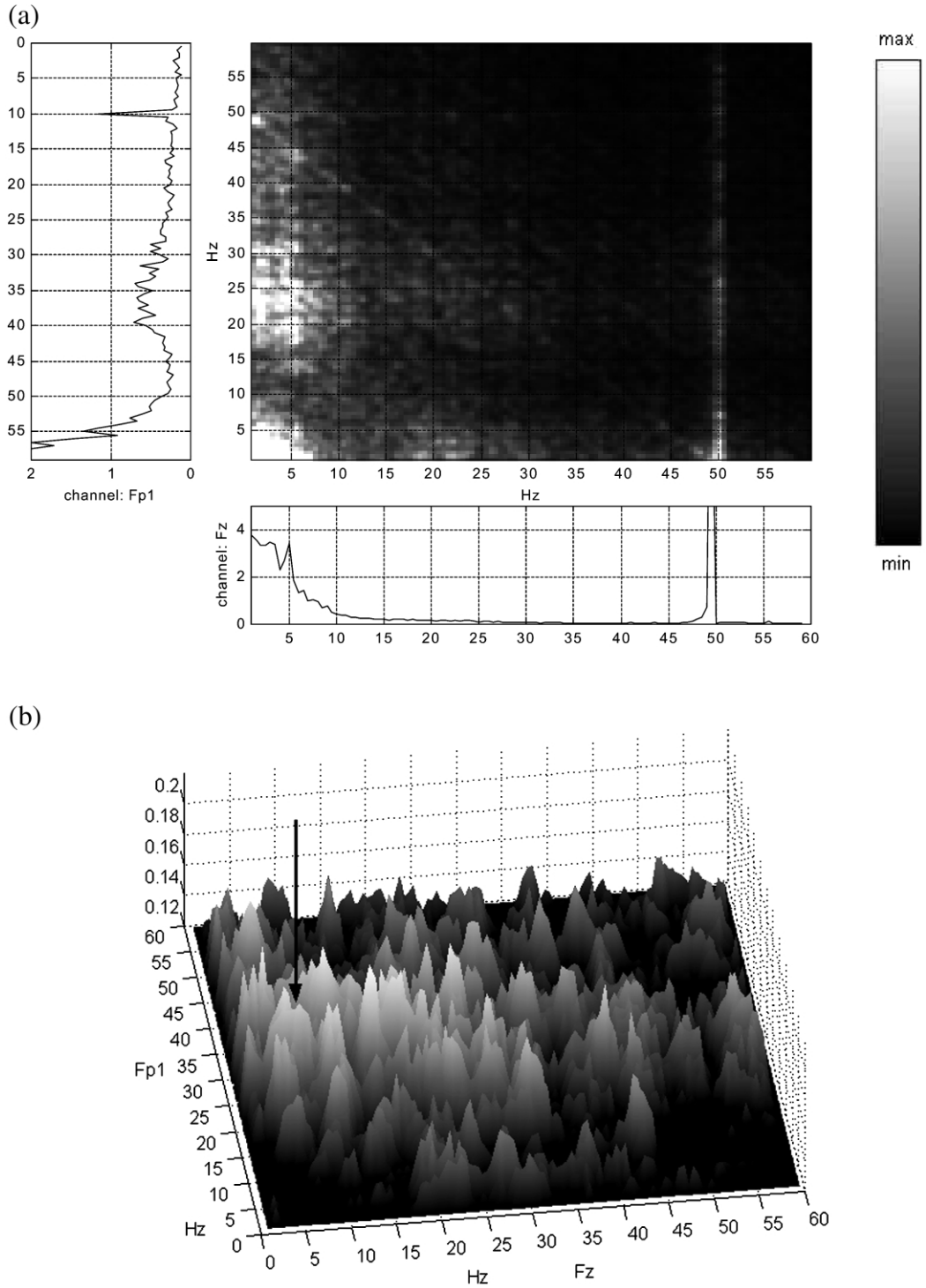

Fig. 6. Cross-bispectral analysis between the triple of channels Fz, Fp1 and Fp1 for one selected subject in case of number word memorising for set size 3 (79 trials): upper panel: cross-biamplitude between Fz and Fp1 and correspondent power spectra (1 selected subject); and lower panel: cross-bicoherence between Fz and Fp1; the arrow points to increased coherence at frequency pair [5 (Fz) and 25 Hz (Fp1)].

quency range 3–7 Hz at Fz and 20–25 Hz at Fp1 by non-linear frequency coupling has to be validated by cross-bicoherence analysis (lower panel of Fig. 6). The arrow marks a high peak around the frequency pair 5 Hz at Fz and 25 Hz at Fp1. The significant difference from zero was tested according to Eq. (6) for all frequency pairs. The significant test results in a matrix of frequency

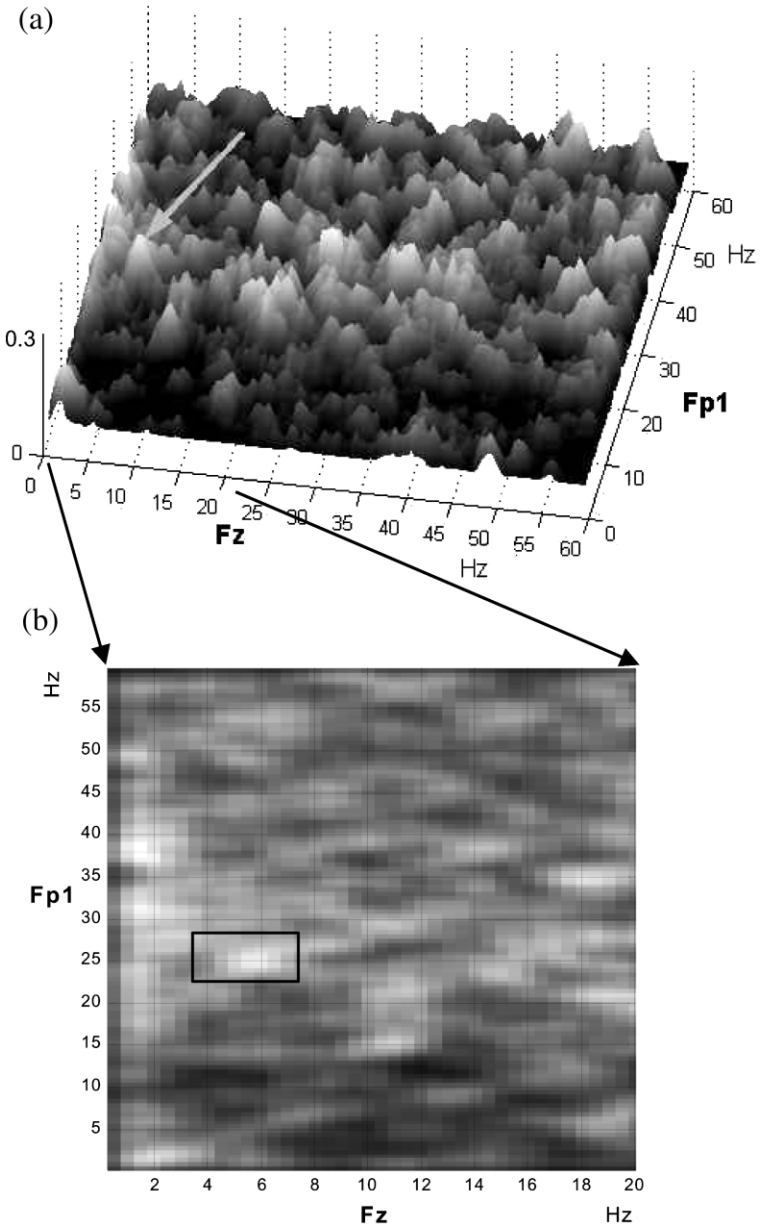

Fig. 7. Upper panel: 3d-presentation of mean test results of non-zero cross-bicoherence (10 subjects) between the triple of channels Fz, Fp1 and Fp1 and correspondent mean power spectra during memorising number words (average of set sizes 3 and 4). The arrow points at the frequency pair of approximately 6 (at Fz) and 25 Hz (at Fp1) with cumulative, significantly high bicoherence. Power panel: 2d-view of the cutting of the upper matrix with frequencies of interest. The region (3–7 Hz) × (24–29 Hz) is marked by a rectangle.

pairs with one in the case of non-zero bicoherence and zero otherwise.

The described analysis was performed for both memorising number words and figures with set sizes 3 and 4 and all four triplets of channels mentioned above. Mean matrices for 10 subjects of test results of non-zero cross-bicoherences indicate possible frequency ranges with non-linear phase coupling. The 3-D view of the mean matrix for memorising number words (average of set sizes 3 and 4) for the triplet of channels (Fz, Fp1 and Fp1) is represented in the upper part of Fig. 7.

High values were obtained within the frequency range 20–35 Hz/20–35 Hz. Since power values at Fz for frequencies larger than 20 Hz are negligible, our interest was focused to the area of low frequencies at Fz and fast frequencies (20–30 Hz) at Fp1. A clear peak at 5 Hz at Fz, and 25 Hz at Fp1 is marked by an arrow.

The lower part of Fig. 7 shows the cutting with frequencies of interest. The main region of interest is marked by a black rectangle. Cumulative phase coupling may be observed also at 2–3 Hz at Fz and 25–40 Hz at Fp1.

The strength of phase coupling was investigated statistically for all frequency regions with high intensity of non-zero cross-bicoherence separately for set sizes 3 and 4, both for memorising number words and figures. Analogously to the approach in Section 3.3.1, the mean percentage (Table 3) of test positivity for non-zero cross-bicoherence were calculated for set size 3 and 4.

The results with frequent appearance of phase coupling are similar for both set sizes. Thus, a randomness of the results may be excluded. For remembering number words the strongest phase-coupling effects were obtained for 3–7 Hz at F3 and Fz, respectively, and for 24–29 Hz at Fp1, but for remembering figures for 1–5 Hz at F3 and Fz, respectively, and for 18–23 Hz at Fp1, and additionally for 1–5 Hz at F4 and Fz, respectively, and for 25–30 Hz at Fp2.

An outstanding result is the strong phase-coupling of slow rhythms (3–7 Hz) at Fz and fast rhythms (24–29 Hz) at Fp1 for remembering number words. Non-zero bicoherence was observed for all 10 subjects for set size 3, and for seven of 10 subjects for set size 4.

3.4. Time-variant coherence between low oscillations and the envelope of fast oscillations

A synchronisation between the EEG at Fz,

Table 3
Mean percentage of test positivity for non-zero cross-bicoherence for selected frequency area [significance test according to Eq. (6) with α-level = 5%]

Frequency area (Hz)	Number words: set size = 3				Random figures: set size = 3			
	Fp1/F3	Fp2/F4	Fp1/Fz	Fp2/Fz	Fp1/F3	Fp2/F4	Fp1/Fz	Fp2/Fz
1–5/18–23	40%	10%	30%	10%	**50%**	30%	**60%**	40%
1–5/25–30	20%	30%	20%	40%	40%	**40%**	20%	**60%**
2–6/29–34	10%	10%	20%	20%	10%	10%	20%	10%
3–7/24–29	**50%**	20%	**100%**	30%	30%	30%	30%	20%
7–12/18–23	30%	30%	30%	30%	60%	10%	30%	20%
7–12/35–40	30%	20%	30%	10%	20%	40%	40%	20%
8–13/33–38	10%	30%	30%	20%	30%	20%	10%	30%
	Number words: set size = 4				Random figures: set size = 4			
1–5/18–23	20%	10%	40%	20%	**50%**	30%	**50%**	30%
1–5/25–30	30%	20%	50%	20%	30%	**40%**	30%	**30%**
2–6/29–34	20%	30%	10%	10%	10%	0%	10%	10%
3–7/24–29	**50%**	30%	**70%**	40%	50%	20%	50%	20%
7–12/18–23	30%	40%	30%	40%	30%	30%	30%	30%
7–12/35–40	20%	20%	50%	0%	30%	30%	50%	20%
8–13/33–38	20%	40%	10%	20%	30%	30%	30%	30%

Table 4
Frequency ranges of fast oscillations at Fp1 for memorising number words

Subject	Frequency range of fast oscillations
1	19–35
2	25–40
3	20–30
4	24–31
5	17.5–27
6	18.5–28
7	21.5–34.5
8	18.5–34
9	14–23
10	19.5–32.5

denoted by $[x^m(t_n)]_{n=0,1,\ldots}$, and the envelope $[e^m(n)=e^m(t_n)]_{n=0,1,\ldots}$ of fast oscillations of the EEG at Fp1, denoted by $[y^m(t_n)]_{n=0,1,\ldots}$, may serve as a possible explanation of non-linear phase coupling between slow oscillations at Fz and fast oscillations at Fp1 for memorising number words. (The value m denotes the number of the single trial, $m = 1,..., M$.)

According to the last chapter the strongest non-linear phase coupling was detected for memorising number words. For this case, the following calculations were performed: the frequency domain with fast oscillations was determined for each subject from their mean power spectra at Fp1. The frequency ranges for each subject are listed in Table 4.

Both the main frequency and the width of the frequency band varied inter-individually. The EEG data at Fp1 for each subject were filtered by a FIR filter (window length = 50) for the correspondent frequency bands. Afterwards, the envelope was calculated according to Eq. (8). The synchronisation between this envelope and the EEG signal at Fz was investigated by means of instantaneous coherence analysis. Additionally, for each subject, mean time–power analysis was performed.

For a better understanding of the results of one subject (the same as in Fig. 6) are presented at first. The upper and middle panels in Fig. 8 show the time–power spectra at Fp1 and at Fp2, respectively, for memorising number words (set size 3).

The time interval of 4200 ms includes the presentation of the second and the third word (0–2400 ms), and the retention period. For Fp1, increased power between 19 and 28 Hz may be observed during the two presentations. With the beginning of the retention period, two distinguishable oscillations, approximately 20 and 26 Hz, emerge (marked with dotted lines -----) very clearly up to 3500 ms. For Fp2 only one frequency band with fast oscillations, approximately 20 Hz, may be observed.

The EEG signal at Fp1 was filtered with a bandpass of 18.5–34 Hz. The instantaneous coherence of the envelope of the filtered signal and the EEG signal at Fz is illustrated in the lower panel of Fig. 8. During the presentation of the two number words, increased coherences appear at approximately 2 and 8 Hz. With the beginning of the retention period, coherence of approximately 6 Hz increases (marked with dotted line -----). This result indicates an amplitude modulation of fast frequencies at Fp1 by slow frequencies at Fz for a time interval of 1000 ms at the beginning of the retention period.

The time–power and time–coherence analysis described for one subject was performed for each subject with its individual fast frequency band (Table 4). Because of the inequality of the individual frequency bands of fast oscillations, a broad mean high power frequency band from 25 Hz up to 35 Hz is the result. The frequency range with high coherence is concentrated approximately 4–8 Hz during retention. The highest frequencies occur at approximately 6 Hz. These results are in accordance with an amplitude modulation model and suggest a functional co-operation between frontopolar regions and Fz during retention, and this in spite of different frequencies in these two regions.

4. Discussion

The results in Section 3 manifest the existence

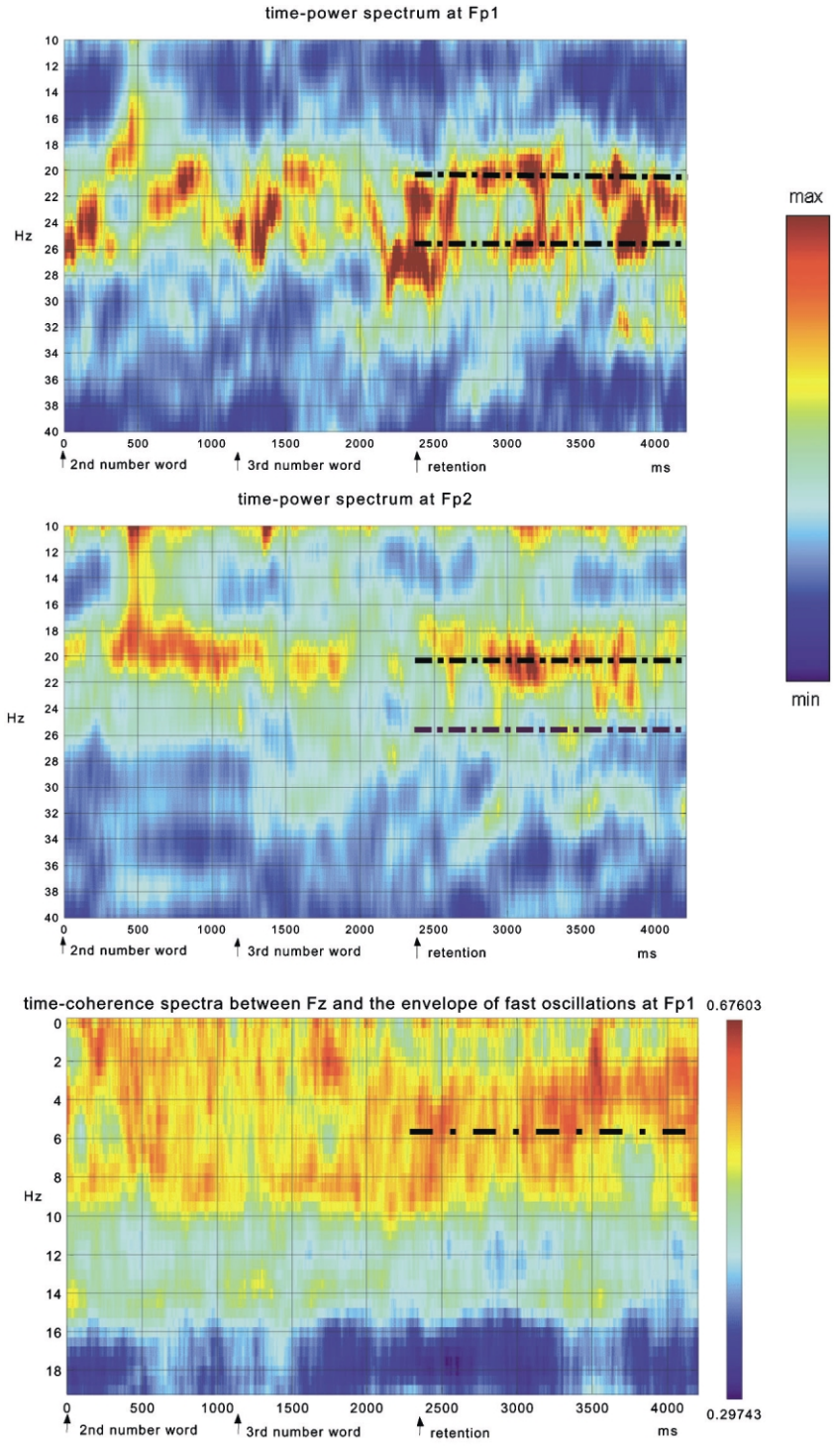

Fig. 8. Mean time–power spectra of one subject (79 trials) at Fp1 (upper panel) and Fp2 (middle panel), and mean instantaneous coherence spectrum between Fz and the envelope of the filtered signal (18.5–34 Hz) at Fp1 (lower panel) during the presentation of the 2nd and the 3rd number word and the retention period for memorising number words (set size 3).

of phase-coupling between theta- and gamma EEG activities during memory processing. Whereas the double peak of fast oscillations with a distance of approximately 5–7 Hz in bicoherence at Fp1, suggests only the presumption of possible phase-coupling (Section 3.3.1), the significantly increased cross-bicoherence between rhythms of 3–7 Hz at F3 and Fz, and 24–29 Hz at Fp1 clearly verifies the existence of theta–gamma phase-coupling (Section 3.3.2). The occurrence of both theta- and gamma activities during memory processing by several authors as mentioned in the introduction could be verified. Moreover, it could be shown that these activities are interdependent in a non-linear way. The instantaneous coherence analysis between the envelope at Fp1 and the raw EEG at Fz point at amplitude modulation as one possible explanation of the generation of non-linear relationships between different rhythms (section 3.4).

The results of phase coupling between theta rhythms at Fz and fast rhythms at the left frontopolar electrode position Fp1 underline the observations of the separation and specification of different prefrontal areas made by several authors (see e.g. Wilson et al., 1993; Goldman-Rakic, 1997). The involvement of the left frontopolar area during memorising number words in particular coincides with the results of Tulving et al. (1994) and Iidaka et al. (1999).

In this respect, the influential work by Fuster (1989) has to be quoted who detected large contingents of prefrontal neurons that undergo sustained activation in delayed-response experiments, i.e. during the period of retention of a cue before the monkey is required to respond. This was shown to be true of both spatially defined and non-spatial information. Thus, in general, the prefrontal cortex evidently plays a critical role in the temporal organisation of behaviour. These and other observations (Isseroff et al., 1982; Goldman-Rakic and Friedman, 1991) substantiate the conclusion that the prefrontal cortex is strongly involved in working memory, i.e. in the constant updating of information. Based on clinical observations, Damasio (1990) considers the dorsolateral region of prefrontal cortex as 'critical for coherent organisation of mental contents on which creative thinking and language depend and that permit, in general, artistic activities and the planning of future activities' (p. 369). Similar inferences were drawn by Petsche and Etlinger (1998) from their observations of the behaviour of prefrontal coherence in the alpha band during different cognitive tasks.

As to the question where the EEG recorded from Fz originates, two regions have to be considered: Brodmans areas 4, 6 and 8; and the cingulate gyri, areas 23 and 24 underneath. Since the EEG findings at Fz in the theta range were shown to be related to memory functions, it is most likely that the cingulate area that is known to play a decisive role in the limbic system underlies it. The other regions beneath Fz are mainly involved in extrapyramidal functions. Thus, the results of this paper can most likely be interpreted as an EEG aspect of the functional linking between prefrontal cortex and the limbic system.

Results with regard to phase-coupling could not be obtained with the same cogency as for remembering number words (see Table 3) for memorising random figures.

Even if these results do not explain the physiological mechanisms underlying these non-linear synchronisation phenomena, they clearly demonstrate the presence of phase-coupled activities. The broader gamma frequency band and the higher main gamma frequency probably are due to non-linear theta-gamma oscillations. This result, among others, shows the limitation of ordinary power analysis which assumes independence of oscillations at different frequencies. Ordinary power analysis cannot distinguish between primary and derived activities by non-linear phase coupling.

Estimating bispectral parameters such as cross-biamplitude and cross-bicoherence is based on the Fourier approach and includes the whole retention period. It is well-known that the Fourier approach presupposes stationarity of the signal and does not allow investigations of temporal changes in interdependencies between different rhythms. The analysis of the relation between the envelope of fast rhythms at Fp1 and the raw EEG

at Fz by means of instantaneous coherence leads one to assume temporal changes of the strength of amplitude modulation (compare Fig. 8).

In the present analysis, we referred to data reflecting processing during retention which has to be considered as a stochastic mixture of processes during retention. For future investigations along this line, psychological results are of particular importance that point to stronger temporal regularities in actual short-term behaviour during retention and recognition. Exploration of these relationships demands new tools for EEG analysis that take temporal short-term dynamics explicitly into account. Temporal regularities have already been obtained in earlier investigations focusing on the Sternberg task as experimental paradigm (Sternberg, 1975; Bredenkamp, 1993; Bredenkamp and Klein, 1998). Psychological studies quoted so far referred solely to the test period of the Sternberg task. Cavanagh's representation of item-specific operation times as segments of a fundamental base period by considering the relation to storage capacity suggests a close connection to cyclic processes during retention as assumed in Lisman's multiplexing hypothesis (Jensen and Lisman, 1996). These findings fit well into the framework of the taxonomic quantum model (TQM) by Geissler (1987, 1991) suggested on the basis of a much broader range of phenomena and for different tasks and criteria of behavioural measurement.

Acknowledgements

The authors would like to thank G. Lueer, U. Lass and D. Becker (Institute of Psychology, University of Goettingen) for their support in the design of the Sternberg task and their helpful discussions. This study was supported by the German Ministry of Research (DFG Scha 741/1-4 and Wi 1166/2-3).

References

Braver, T.S., Cohen, J.D., Nystrom, L.E., Jonides, J., Smith, E.E., Noll, D.C., 1997. A parametric study of prefrontal cortex involvement in human working memory. Neuroimage 5, 49–62.

Bredenkamp, J., 1993. The relations between various invariance hypotheses in the psychology of memory. Z. Exp. Angewandte Psychol XI (3), 368–385. (in German).

Bredenkamp, J., Klein, K.-M., 1998. Experimental tests of a model connecting three invariance hypotheses on learning and memory processes. Z. Psychol. 206, 107–124.

Cabeza, R., Nyberg, L., 1997. Imaging cognition: an empirical review of PET studies with normal subjects. J. Cogn. Neurosci. 9, 1–26.

Cavanagh, J.P., 1972. Relation between the immediate memory span and the memory search rate. Psychol. Rev. 79, 525–530.

Bullock, T.H., Achimowicz, J.Z., Duckrow, R.B., Spencer, S.S., Iragui-Madoz, V.J., 1997. Bicoherence of intracranial EEG in sleep, wakefulness and seizures. Electroencephalogr. Clin. Neurophysiol. 103, 661–678.

Damasio, A.R., 1990. Synchronous activation in multiple cortical regions: a mechanism for recall. Semin. Neurosci. 2, 287–296.

Eckhorn, R., Frien, A., Bauer, R., Woelbern, T., Kehr, H., 1993. High frequencies (60–90 Hz) oscillations in primary visual cortex of awake monkey. Neuroreport 4, 243–246.

Fernandez, G., Effern, A., Grunwald, Th. et al., 1999. Real-time tracking of memory formation in the human rhinal cortex and hippocampus. Science 285, 1582–1585.

Fuster, J.M., 1989. The Prefrontal Cortex, 2nd ed. Raven Press, New York.

Gajraj, R.J., Doi, M., Mantzaridis, H., Kenny, G.N.C., 1998. Analysis of the EEG bispectrum, auditory evoked potentials and the EEG power spectrum during repeated transitions from consciousness to unconsciousness. Br. J. Anaesth. 80, 46–53.

Geissler, H.-G., 1987. The temporal architecture of central information processing: evidence for a tentative time–quantum model. Psychol. Res. 49, 99–106.

Geissler, H.-G., 1991. Zeitcodekonstanten-ein Bindeglied zwischen Psychologie und Physiologie bei der Erforschung kognitiver Prozesse? Hypothesen und Überlegungen zu Quantenstrukturen in der Alphaaktivität des Gehirns. Z. Psychol. 199 (2), 121–143.

Geissler, H.-G., 1997. Is there a way from behavior to non-linear brain dynamics? On quantal periods in cognition and the place of alpha in brain resonances. Int. J. Psychophysiol. (Special Issue) 26, 381–393.

Geissler, H.-G., Schebera, F.-U., Kompass, R., 1999. Ultra-precise quantal timing: evidence from simultaneity thresholds in long-range apparent movement. Percept. Psychophys. 61 (4), 707–726.

Gevins, A., Smith, E.S., McEvoy, L., Daphne, Yu., 1997. High-resolution EEG Mapping of cortical activation related to working memory: effects of task difficulty, type of processing, and practice. Cereb. Cortex 7, 374–385.

Goldman-Rakic, P., 1988. Topography of cognition: parallel distributed networks in primate association cortex. Ann. Rev. Neurosci. 11, 137–156.

Goldman-Rakic, P.S., Friedman, H.R., 1991. The circuitry of working memory revealed by anatomy and metabolic imaging. In: Levin, H.S., Eisenberg, H., Benton, A.L. (Eds.), Frontal Lobe Function and Dysfunction. Oxford University Press, New York-Oxford, pp. 72–91.

Goldman-Rakic, P., 1997. Space and time in the mental universe. Nature 386, 559–560.

Grieszbach, G., Schack, B., Putsche, P., Bareshova, E., Bolten, J., 1994. The dynamic description of a stochastic signal by its adaptive momentary power and momentary frequency estimation and its application to biological signals. Med. Biol. Eng. Computing 32 (6), 632–637.

Iidaka, T., Sadato, N., Yamada, H., Yonekura, Y. 1999. Functional asymmetry of human prefrontal cortex in verbal and non-verbal episodic memory as revealed by fMRI. Cog. Brain Res. (in press).

Isseroff, A., Rosvold, H.E., Galkin, T.W., Goldman-Rakic, P.S., 1982. Spatial memory impairment following damage to the mediodorsal nucleus of the thalamus in rhesus monkeys. Brain Res. 232, 107–113.

Jeffrey, C.S., Chamoun, N.G., 1994. An introduction to bispectral analysis for the electroencephalogram. J. Clin. Monit. 10, 392–404.

Jensen, O., Lisman, J.E., 1996. Novel lists of 7 ± 2 known items can be reliably stored in an oscillatory short-term memory network: interaction with long-term memory. Learn. Mem. 3, 257–263.

Jensen, O., Lisman, J.E., 1998. An oscillatory short-term memory buffer model can account for data on the Sternberg task. J Neurosci. 18, 10688–10699.

Joliot, M., Ribary, U., Llinas, R., 1994. Human oscillatory brain activity near 40 Hz co-exists with cognitive temporal binding. Proc. Natl. Acad. Sci. 91, 11748–11751.

Kim, S.B., Powers, E.J., 1979. Digital bispectral analysis and its applications to non-linear wave interactions. IEEE Trans. Plasma Sci. 7, 120–131.

Klimesch, W., 1996. Memory processes, brain oscillations and EEG synchronisation. Int. J. Psychophys. 24, 61–100.

Klimesch, W., Doppelmayr, M., Schimke, H., Ripper, B., 1997. Theta synchronisation and alpha desynchronisation in a memory task. Psychophysiology 34, 169–176.

Klimesch, W., 1999. EEG alpha and theta oscillations reflect cognitive and memory performance: a review and analysis. Brain Res. Rev. 29, 169–195.

Lisman, J.E., Idiart, M.A.P., 1995. Storage of 7 ± 2 short-term memories in oscillatory subcycles. Science 267, 1512–1515.

Llinas, R., Ribary, U., Contreras, D., Pedroarena, C., 1998. The neuronal basis for consciousness. Phil. Trans. R. Soc. Lond. B 353, 1841–1849.

Miller, R., 1991. Cortico-Hippocampal Interplay and the Representation of Contexts in the Brain. Springer, Berlin.

Möller, E., Schack, B., Grießbach, G., Witte, H., 1999. Mean, parametric, time-dependent spectral analysis of event-related potentials. Med. Biol. Eng. Comput. 37 (Supplement 2), 420–421.

Möller, E., Schack, B., Arnold, M., Witte, H., 2001. Instantaneous EEG coherence analysis by means of adaptive high-dimensional autoregressive models. J. Neurosci. Methods 105, 143–158.

Muthuswamy, J., Sherman, D.L., Thakor, N.V., 1999. Higher-order Spectral Analysis of Burst Patterns in EEG. IEEE Trans. Biomed. Eng. 46, 92–98.

Nakamura, K., Mikami, A., Kubota, K, 1992. Oscillatory neuronal activity related to visual short-term memory in monkey temporal pole. Neuroreport 3, 117–120.

Nikias, L.Ch., Petropulu, A.P., 1993. Higher-Order Spectra Analysis. PTR Prentice Hall, Englewood Cliffs, New Jersey, USA.

Paulesu, E., Frith, C.D., Frackowiak, R.S.J., 1993. The neural correlates of the verbal component of working memory. Nature 362, 342–345.

Petrides, M., Alivasatos, B., Meyer, E., Evans, A.C., 1993. Functional activation of the human frontal cortex during the performance of verbal working memory task. Proc. Natl. Acad. Sci. 90, 878–882.

Petsche, H., Etlinger, S.C., 1998. EEG and Thinking: Power and Coherence Analysis of Cognitive Processes. Austrian Academy of Sciences, Vienna 383 pp.

Sarnthein, J., Petsche, H., Rappelsberger, P., Shaw, G.L., von Stein, A., 1998. Synchronisation between prefrontal and posterior association cortex during human working memory. Proc. Natl. Acad. Sci. USA 95, 7092–7096.

Schack, B., Grießbach, G., Krause, W., 1999a. The sensitivity of instantaneous coherence for considering human information processing. Part I: the relationship between mental activities and instantaneous EEG coherence. Int. J. Psychophys. 31, 219–240.

Schack, B., Grießbach, G., Nowak, H., Krause, W., 1999b. The sensitivity of instantaneous coherence for considering human information processing. Part II: similarities and differences between EEG and MEG coherences. Int. J. Psychophys. 31, 241–259.

Schack, B., Chen, A.C.N., Mescha, S., Witte, H., 1999c. Instantaneous EEG coherence analysis during the stroop task. Clin. Neurophysiol. 110, 1410–1426.

Schack, B., Rappelsberger, P., Anders, Ch., Weiss, S., Möller, E., 2000. Int. J. Bifurcation Chaos 10, 2565–2586.

Schanze, T., Eckhorn, R., 1997. Phase correlation among rhythms present at different frequencies: spectral methods, application to microelectrode recordings from visual cortex and functional implications. Int. J. Psychophys. 26, 171–189.

Shallice, T., Fletcher, P., Frith, C.D., Grasby, P., Frackowiak, R.S.J., Dolan, R.J., 1994. Brain regions associated with acquisition and retrieval of verbal episodic memory. Nature 368, 633–635.

Shils, J.L., Litt, M., Skolnick, B.E., Stecker, M.M., 1996. Bispectral analysis of visual interactions in humans. Electroencephalogr. Clin. Neurophysiol. 98, 113–125.

Singer, W., 1993. Synchronisation of cortical activity and ist putative role in information processing and learning. Annu. Rev. Physiol. 55, 349–374.

Smith, E.E., Jonides, J., Koeppke, R.A., 1996. Dissociating verbal and spatial working memory using PET. Cerebral Cortex 6, 11–20.

Squire, L.R., Ojemann, J.G., Miezin, F.M., Petersen, S.E., Videen, T.O., Raichle, M.E., 1992. Activation of the hippocampus in normal humans: a functional anatomical study of memory. Proc. Natl. Acad. Sci. USA 89, 1837–1841.

Sternberg, S., 1975. Memory scanning: new findings and current controversies. Q. J. Exp. Psychol. 27, 1–32.

Swartz, B.E., Halgreen, E., Fuster, J.M., Simpkins, E., Gee, M., Mandelkern, M., 1991. Cortical metabolic activation in humans during a visual memory task. Cereb. Cortex 5, 205–214.

Tallon-Baudry, C., Bertrand, O., Delpuech, C., Pernier, J., 1997. Oscillatory gamma-band activity induced by a visual search task in humans. J. Neurosci. 17, 722–734.

Tallon-Baudry, C., Bertrand, O., Peronnet, F., Pernier, J., 1998. Induced gamma-band activity during the delay of a visual short-term memory task in humans. J. Neurosci. 18, 4244–4254.

Tallon-Baudry, C., Bertrand, O., 1999. Oscillatory gamma activity in humans and ist role in object representation. Trends Cognit. Sci. 3, 151–162.

Tulving, E., Kapur, S., Craik, F.I.M., Moscovitch, M., Houle, S., 1994. Hemispheric encoding/retrieval asymmetry in episodic memory: positron emission tomography findings. Proc. Natl. Acad. Sci. USA 91, 2016–2020.

Wilson, A.W., O Scalaidhe, S.P., Goldman-Rakic, P.S., 1993. Dissociation of object and spatial processing domains in primate prefrontal cortex. Science 260, 1955–1958.